INTERNATIONAL JOURNAL FOR NUMERICAL METHODS IN FLUIDS, VOL. 15, 1197–1212 (1992)

THEORETICAL INVESTIGATION OF COMBUSTION CHARACTERISTICS IN RAM-JET DUMP COMBUSTOR WITH SIDE-INLET

SHU-HAO CHUANG

Department of Mechanical Engineering, National Chung-Hsing University, Taichung, Taiwan 402, R.O.C.

HSUN-CHENG LIN

Department of Mechanical Engineering, Shu-Teh Junior College of Technology, Taichung, Taiwan 402, R.O.C.

MING-HUA CHEN

Department of Mechanical Engineering, Chung-Chou Institute of Technology, Chunghuax, Taiwan 510, R.O.C.

AND

JIN-FA JAN

Graduate School of Mechanical Engineering, Feng-Chia University, Taichung, Taiwan 407, R.O.C.

SUMMARY

The combustion flow of a sudden-expansioin dump combustor with injecting side-inlet is analysed using the SIMPLE-C algorithm and the Jones–Launder k–ε two-equation turbulence model. The transport properties of velocity, turbulence kinetic energy, temperature and combustion efficiency as a function of the injected mass fraction and the number of side-inlet nozzles are solved in this paper. The axial velocities of the sudden-expansion dump combustor without injected side-inlet flow are solved first and found to be in good agreement with the experimental data of Moon and Rudinger. For a fixed value of the side-inlet number the wall temperature and combustion efficiency of the dump combustor are decreased when the injected mass fraction is increased. For a fixed value of the injected mass fraction the wall temperature and combustion efficiency are decreased when the number of side-inlet nozzles is increased.

KEY WORDS Combustion flow Combustor Side-inlet Numerical calculation SIMPLE-C algorithm

INTRODUCTION

The flow field in an annular combustion chamber with one or more side-inlet jets of cooling air injected is very complicated since it is characterized by a synthesis of a number of diverse flow regions. These flow regions are the inlet jets, the jet–cross-flow collision, the recirculating flow and the developing flow far downstream of the combustor inlet. The side-inlet flow plays an important role in the enhancement of combustion performance in a gas turbine combustor. In the primary zone it serves to increase mixing and combustion efficiency, to eliminate the formation of pullutants and to stabilize the flame. It can also accelerate soot oxidation in the intermediate zone and render a uniform outlet temperature distribution to avoid the occurrence of hot spots in the

0271–2091/92/221197–16$13.00

Received October 1991
Revised May 1992

dilution zone.[1] Therefore a better understanding of this flow field is highly desirable. In particular, the injected mass fraction and the number of side-inlet jets have a great effect in determining combustion performance. One or more side-inlet jets injected normally into a non-swirling cross-flow is the focus of the present study. The aim of the current study is to show how the structure of the recirculation zone and the combustion efficiency of the dump combustor are affected by the introduction of side-inlet flow into the combustion chamber.

The literature reports both theoretical and experimental studies of the effects of uniform cross-flow on jet flows had been studied.[2-6] Patankar *et al.*[2] analysed the effect of a single jet in an unconfined cross-flow by a numerical method. Chassaing *et al.*[3] and Crabb *et al.*[4] made detailed measurements of the velocity field with its associated turbulence and vortex pair by utilizing laser–Doppler velocimetry (LDV). Opposed jets in a uniform cross-flow were studied by Atkinson *et al.*[5] experimentally. The numerical simulation of twin-jet impingement on a flat plate coupled with cross-flow was studied by Chuang *et al.*[6] These results showed good agreement between the numerical predictions and experimental data. Side-inlet jets in gas turbine combustor flows have also been studied.[7-13] Shahaf *et al.*[7] first conducted an investigation of the two-dimensional mean flow field in a square cross-sectional channel with two side-inlets, both analytically and experimentally. Large discrepancies between the measured and calculated axial mean velocity profiles were found along the channel axis and in the recirculation region. Choudhury[8] experimentally tested the combustor performance of a gas generator ram-jet with four side-inlets and concluded that the inlet flow angle does not have any influence on the recirculating zone in the head region of the combustor. Vanka *et al.*[9,10] calculated the three-dimensional mean flow field in a cylinder combustor with two side-inlets separated by an azimuthal angle of 90°. They found an optimal head height for the best combustion efficiency. The distributions of velocity, temperature and concentration at the combustor outlet when a side-inlet jet was introduced into a swirling flow field were calculated and studied by Serag-Eldin and Spalding[11] and Shyy *et al.*[12] The effect of wall injection flow on the size and shape of the swirl-induced central recirculation zone was investigated by Kilik and Schmidt.[13] However, most of the above researchers have no experimental data to validate the turbulence and combustion models used in their calculations. In view of the lack of quantitative experimental data with which to compare numerical predictions, several workers[14-19] performed detailed measurements of one or more opposed wall jets injected into confined swirling and non-swirling cross-flows.

Previous work on the simulation of combustor flow fields utilized the streamfunction–vorticity method and the k–ε two-equation turbulence model to analyse a two-dimensional combustor.[20] There have also been studies of combustor flow using p–u–v primitive variables and the k–ε turbulence model.[21-27] The process incorporated the SIMPLE algorithm technique initiated by Patankar.[28] The SIMPLE-C algorithm developed by van Doormaal and Raithby[29] and Latimer and Pollard[30] has a better convergence rate of residual mass[31] than that of the SIMPLE algorithm. However, the above studies were limited to reacting flow in a dump combustor with side-inlet and did not consider the cooling effects of the injecting side-inlet. The intention here is to investigate the phenomena of reacting flow in a dump combustor with cooling fluids from the side-inlet. This paper adopts the SIMPLE-C algorithm and the k–ε turbulence model to study the cooling effect of side-inlet jets on the combustor flow. The finite difference equations are derived by integrating the governing equations over a control volume surrounding each grid point. A power-law scheme[28] is used for the representation of the convective and diffusive terms across the control surface.

GOVERNING EQUATIONS AND TURBULENT COMBUSTION MODEL

The combustion flow analysis of the sudden-expansion dump combustor with side-inlet flow is very complicated. In order to simplify the problem and facilitate the numerical analysis, we make the following assumptioins.

1. The flow field is two-dimensional axisymmetrical.
2. The flow is steady state; the wall of the combustor is adiabatic.
3. Radiation and gravity effects are negligible.
4. The flow field is composed of a single-phase gaseous flow, i.e. we do not consider a two-phase flow problem.
5. The chemical reaction is one-step and has an infinitely fast reaction rate.
6. The effect of density fluctuations is negligible.
7. The Lewis number is equal to unity and the specific heat at constant pressure is a constant.

For the steady axisymmetric turbulent flow the general form of the transport equatioin can be written as

$$\underbrace{\frac{1}{r}\left[\frac{\partial}{\partial x}(\rho u r\phi)+\frac{\partial}{\partial r}(\rho v r\phi)\right]}_{\text{convection term}}-\underbrace{\frac{\partial}{\partial x}\left(r\Gamma_\phi\frac{\partial\phi}{\partial x}\right)-\frac{\partial}{\partial r}\left(r\Gamma_\phi\frac{\partial\phi}{\partial r}\right)}_{\text{diffusion term}}=S^\phi, \tag{1}$$

where x is the co-ordinate in the axial direction, r is the co-ordinate in the radial direction, ϕ stands for the dependent variables (u, v, k, ε, m_{fo}, H), Γ_ϕ is the appropriate effective exchange coefficient for the turbulent flow and S^ϕ is the source term of the transport equation for ϕ, as shown in Table I. The total effective viscosity of the flow field is

$$\mu_e=\mu_l+\mu_t, \tag{2}$$

Table I. Governing equation variables

ϕ	Γ_ϕ	S^ϕ
u	μ_e	$-\frac{\partial P}{\partial x}+\frac{\partial}{\partial x}\left(\mu_e\frac{\partial u}{\partial x}\right)+\frac{1}{r}\frac{\partial}{\partial r}\left(r\mu_e\frac{\partial v}{\partial x}\right)$
v	μ_e	$-\frac{\partial P}{\partial r}-\frac{2\mu_e v}{r^2}+\frac{\partial}{\partial x}\left(\mu_e\frac{\partial u}{\partial r}\right)+\frac{1}{r}\frac{\partial}{\partial r}\left(r\mu_e\frac{\partial v}{\partial r}\right)$
k	μ_e/σ_k	$\mu_e\left\{2\left[\left(\frac{\partial u}{\partial x}\right)^2+\left(\frac{\partial v}{\partial r}\right)^2+\left(\frac{v}{r}\right)^2\right]+\left(\frac{\partial u}{\partial r}+\frac{\partial v}{\partial x}\right)^2\right\}-\rho\varepsilon$
ε	μ_e/σ_ε	$\frac{C_1\varepsilon}{k}\mu_e\left\{2\left[\left(\frac{\partial u}{\partial x}\right)^2+\left(\frac{\partial v}{\partial r}\right)^2+\left(\frac{v}{r}\right)^2\right]+\left(\frac{\partial u}{\partial r}+\frac{\partial v}{\partial x}\right)^2\right\}-\frac{C_2\rho\varepsilon^2}{k}$
m_{fo}	μ_e/σ_{fo}	0
m_{fu}	μ_e/σ_{fu}	m'_{fu}
H	μ_e/σ_h	0

C_1	C_2	C_μ	σ_k	σ_ε	σ_{fo}	σ_{fu}	σ_h
1·42	1·92	0·09	1·0	1·3	0·9	0·9	0·9

where μ_l and μ_t represent the molecular and eddy viscosity respectively and μ_t is known from the k–ε turbulence model as

$$\mu_t = C_\mu \rho k^2/\varepsilon, \tag{3}$$

with $C_\mu = 0{\cdot}09$ a constant of the model.

In the present analysis CH_4 is used as the fuel and thus the chemical reaction equation can be written as

$$CH_4 + 2(O_2 + 3{\cdot}76N_2) \rightarrow CO_2 + 2H_2O + 7{\cdot}52N_2 + \Delta H_{fu}. \tag{4}$$

The assumption of an infinitely fast chemical reaction rate implies that fuel and oxidant will not coexist at the same time. Therefore the following relations exist in the flow field:

(i) $m_{fu} = 0$ and $m_{ox} = 0$ when $m_{fo} = 0$
(ii) $m_{fu} = 0$ and $m_{ox} = m_{fo}$ when $m_{fo} > 0$
(iii) $m_{ox} = 0$ and $m_{fu} = -(1/s)m_{fo}$ when $m_{fo} < 0$
(iv) $m_{fu} + m_{ox} + m_{pr} = 1$

where $m_{fo} = m_{ox} - s m_{fu}$.

NUMERICAL ANALYSIS AND BOUNDARY CONDITIONS

Grid system

The staggered grid arrangement of integration over the control volume was used to avoid wavy phenomena.[6,28] For the present problem the arrangements of the grid system are optimum when we select 52×22 and 60×22 grid points for cold and reacting flow respectively after checking the accuracy of the grids and the convergence rate.

Finite difference equations

Integration over the control volume and a power-law scheme are employed to construct the finite difference equations. First, integration over the control volume for equation (1) gives

$$J_e A_e - J_w A_w + J_n A_n - J_s A_s = \int\int_v \int S^\phi \, dV, \tag{5}$$

where

$$J_i A_i = \left[(\rho u \phi)_i - \left(\Gamma_\phi \frac{\partial \phi}{\partial x} \right)_i \right] A_i, \qquad i = e, w, n, s.$$

The source term on the RHS of equation (5) was linearized as[6,28]

$$\int\int_v \int S^\phi \, dV = S_p^\phi \phi_p + S_c^\phi \tag{6}$$

where S_p^ϕ and S_c^ϕ are the coefficients of the linearized source term. After the source term has been linearized, equation (5) can be rewritten as

$$a_P^\phi \phi_P = a_E^\phi \phi_E + a_W^\phi \phi_W + a_S^\phi \phi_S + a_N^\phi \phi_N + S_c^\phi, \tag{7}$$

where

$$a_P^\phi = a_E^\phi + a_W^\phi + a_S^\phi + a_N^\phi - S_p^\phi.$$

Table II. Underrelaxation factors f

Cold flow	u	v	k	ε	Γ	P'			
	0·3	0·3	0·5	0·5	0·8	0·8			
Reacting flow	u	v	k	ε	Γ	P'	m_{fo}	H	ρ
	0·2	0·2	0·2	0·5	0·2	0·8	0·3	0·3	0·1

The finite difference equations for u and v were obtained in the same manner as that used for obtaining equation (7), the finite difference equation of ϕ. After integrating the axial and radial momentum equations over the control volume, the following two finite difference equations for u and v were obtained:

$$a_P^u u_P = \sum a_{nb} u_{nb} + S_c^u + (P_P - P_E) A_e, \tag{8}$$

$$a_P^v v_P = \sum a_{nb} v_{nb} + S_c^v + (P_P - P_N) A_n, \tag{9}$$

Solution technique

The SIMPLE-C[29-31] (semi-implicit-pressure-linked-equations-consistent) algorithm was employed to solve the present problem. The solution procedure is initiated with guesses for the velocity and pressure fields and then proceeds with line-by-line iteration. After each sweep over the solution domain, adjustments for the pressure and velocity fields are made to satisfy the continuity equation along each line of the control volume. Further iterations are continued until the continuity equation is satisfied to the convergence criterion. The tolerance of the normalized mass residual is typically between 5×10^{-4} and 10^{-3}. The other dependent variables (k, ε, m_{fo}, H) are also solved line-by-line simultaneously with the mean velocity distribution. In order to avoid numerical instability, an underrelaxation factor is used in the calculation procedure. The underrelaxation factors used in the present calculations are shown in Table II.

Boundary conditions

1. At the inlet: $u = U_{in}$, $v = 0$, $k_{in} = 0{\cdot}003\, U_{in}^2$ and $\varepsilon_{in} = C_\mu k_{in}^{3/2}/(0{\cdot}03\, D/2)$. The inlet velocity of fuel injection was determined by the air–fuel mass ratio, and $m_{fo} = 1$, $m_{fu} = 0$ in the region of the air inlet, $m_{fo} = -s$, $m_{fu} = 1$ in the region of the fuel inlet.
2. At the centreline: $v = 0$ and $\partial\phi/\partial r = 0$ ($\phi = u$, k, ε, P', m_{fo}, H).
3. At the wall: $u = 0$, $v = 0$ (no-slip conditions) and k and ε were handled by the wall function.[32]
4. At the exit: $v = 0$ and $\partial\phi/\partial x = 0$ ($\phi = u$, k, ε, P', m_{fo}, H).
5. At the side-inlet: $u = 0$, $k = 0$, $\varepsilon = 0$ and the radial velocity of the side-inlet was determined by the injected mass fraction.

RESULTS AND DISCUSSION

The flow field conditions used are shown in Table III. This study initially simulates the effects of cooling fluid injected by side-inlet flow on the isothermal sudden-expansion cmbustor. In the reacting flow the drop in the wall temperature and combustion efficiency, which are affected by the injected side-inlet flow, are also calculated. The physical variables adopted in this paper include the number of side-inlet nozzles, the injected mass fraction and the air–fuel ratio. The

Table III. Flow field conditions

Diameter of combustor, D	0·16 m
Diameter of combustor inlet, D_i	0·088 m
Length of combustor, L_c	0·8 m
Reynolds number based on D_i and U_{in}	$3{\cdot}5 \times 10^5$
Air density, ρ	1·211 kg m^{-3}
Air viscosity, μ	$1{\cdot}85 \times 10^{-5}$ kg m^{-1} s^{-1}
Pressure of combustor inlet, P_{in}	1×10^5 N m^{-2}
Temperature of combustor inlet, T_{in}	300 K
Axial velocity of combustor inlet, U_{in}	40 m s^{-1}
Air–fuel ratio, A/F	17·24
Fuel	CH_4

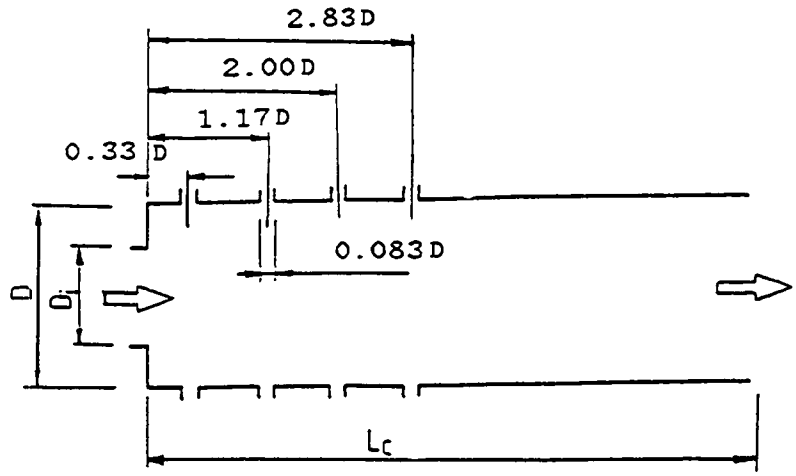

Figure 1. The geometry of the physical plane

configuration of the physical plane is shown in Figure 1. The axial velocities of the sudden-expansion dump combustor without injected side-inlet flow are solved first and found to be in good agreement with the experimental data of Moon and Rudinger[33] as shown in Figure 2.

Effect of $\dot{M}/\dot{M}_o$ on velocity field

The streamlines of the flow field for $\dot{M}/\dot{M}_o = 5\%$, 10%, 15% and 20% in cold flow are shown in Figure 3. It is clearly seen that the corner recirculation zone is affected by side-inlet flow. When the injected mass fraction ($\dot{M}/M_o$) is 5%, the side-inlet flow has no obvious influence on the structure of the corner recirculation zone. However, when $\dot{M}/M_o = 10\%$, the corner recirculation zone becomes smaller and the reattachment point moves upstream as a result of the increased kinetic energy injected from the side-inlet, although the structure of the corner recirculation zone is obviously not destroyed yet. When $\dot{M}/\dot{M}_o = 15\%$, the structure of the corner recirculation zone is obviously changed and the centre of the recirculation zone moves dramatically rightwards, which causes the reattachment point to move downstream. This result is due to the fact that the

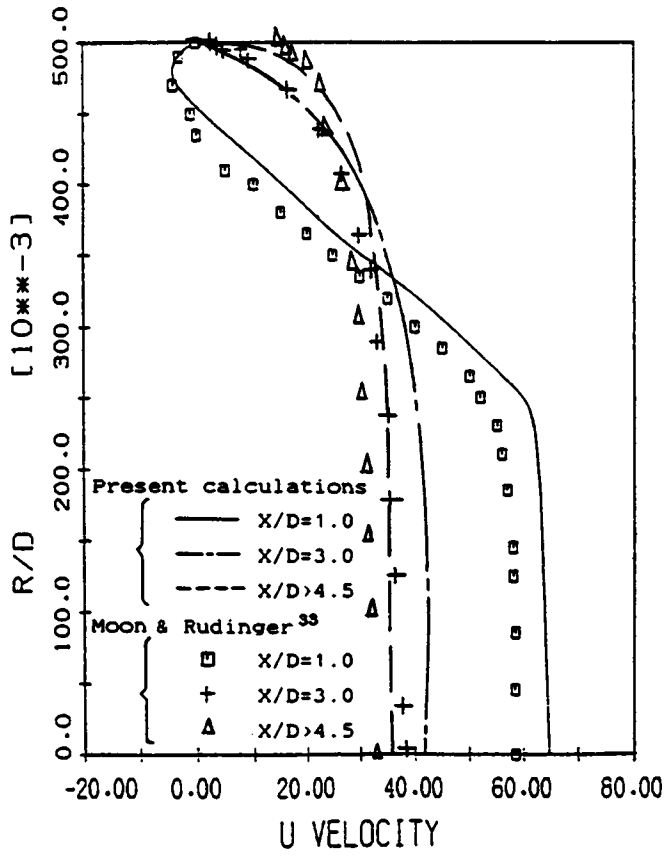

Figure 2. Comparison of predicted and measured axial velocity profiles

induced additional recirculating flow beside the side-inlet exit is promoted and coupled with the primary circulating flow behind the combustor dump step, so that the location of the reattachment point is delayed. When $\dot{M}/\dot{M}_0 = 20\%$, the corner recirculation zone is fully destroyed and there are two recirculation zones which are separatley re-formed on both sides of the side-inlet exit, producing vortex flow in the opposite rotation direction.

Effect of $\dot{M}/\dot{M}_0$ on the turbulence kinetic energy distribution

The turbulence kinetic energy distributions for $\dot{M}/\dot{M}_0 = 5\%$, 10%, 15% and 20% in cold flow are shown in Figure 4. From this figure we find that the turbulence kinetic energy distribution throughout the cold flow is slightly expanded downstream when $\dot{M}/\dot{M}_0$ is increased; this result is due to the fact that a higher injected mass fraction (i.e. greater side-inlet velocity) causes better turbulent mixing.

Effect of $\dot{M}/\dot{M}_0$ on temperature distribution

The temperature distributions for different injected mass fractions in reacting flow when $A/F = 17{\cdot}24$ (i.e. the stoichiometric fuel ratio) are shown in Figure 5. We find that the maximum

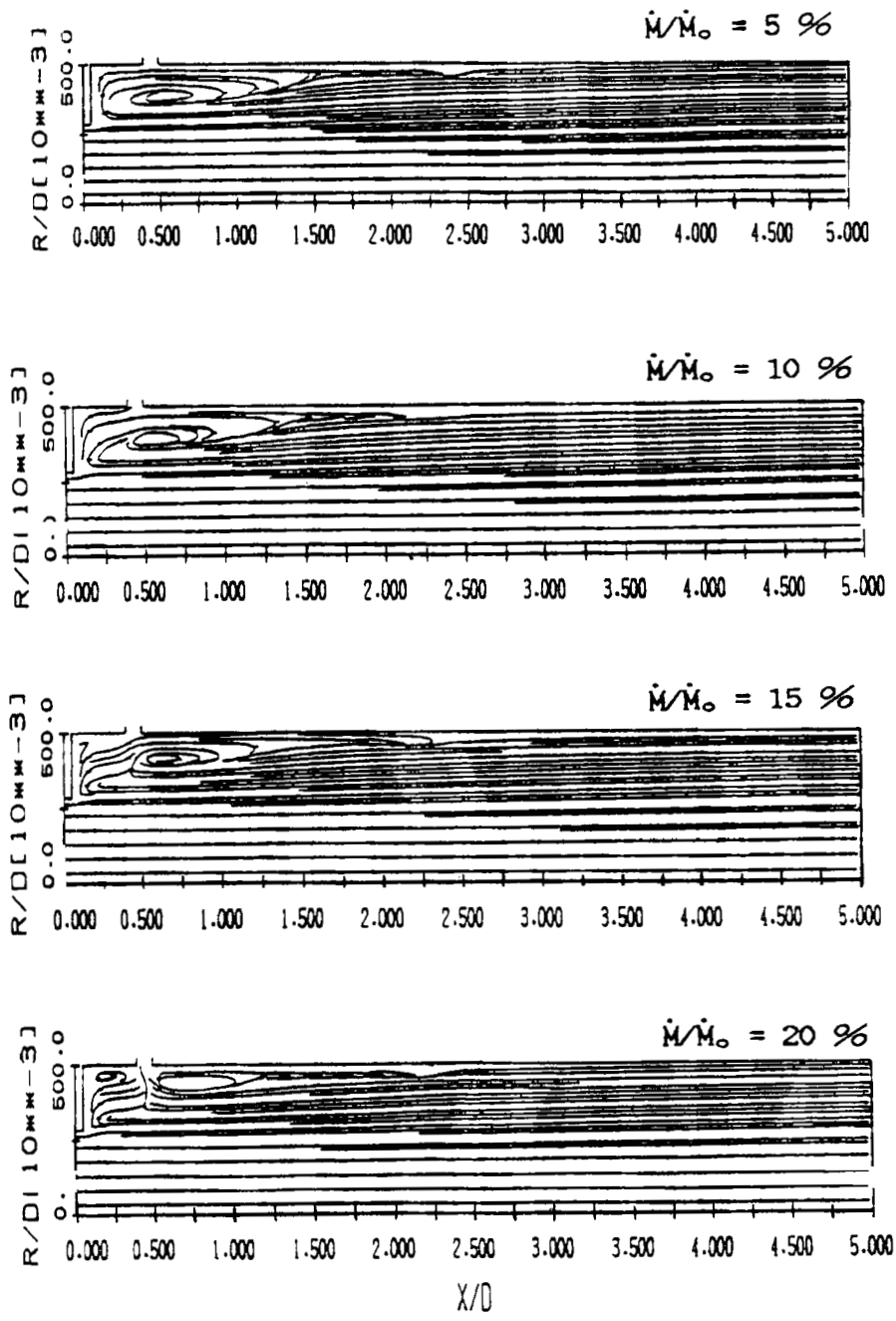

Figure 3. Streamlines for different injected mass fractions

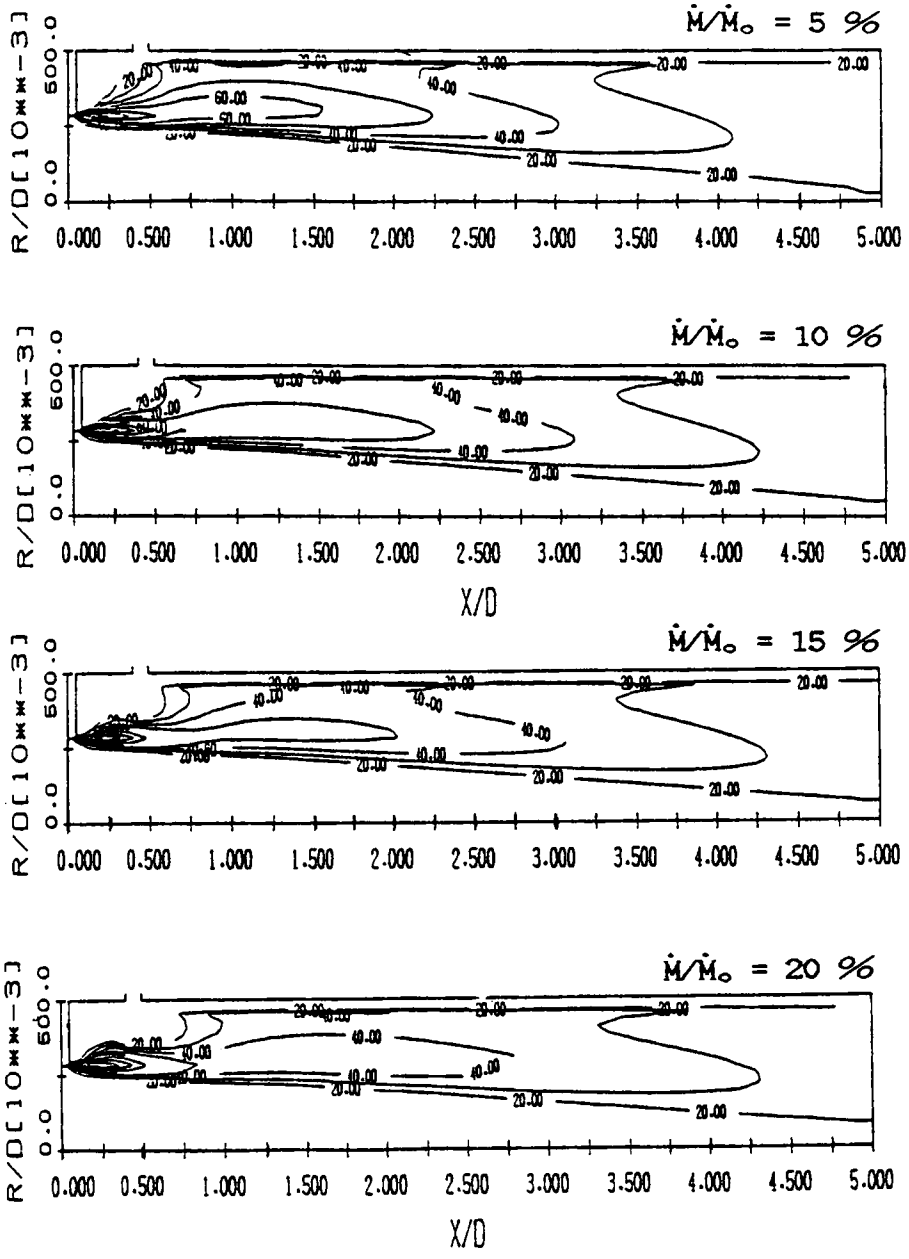

Figure 4. Turbulence kinetic energy distributions for different injected mass fractions

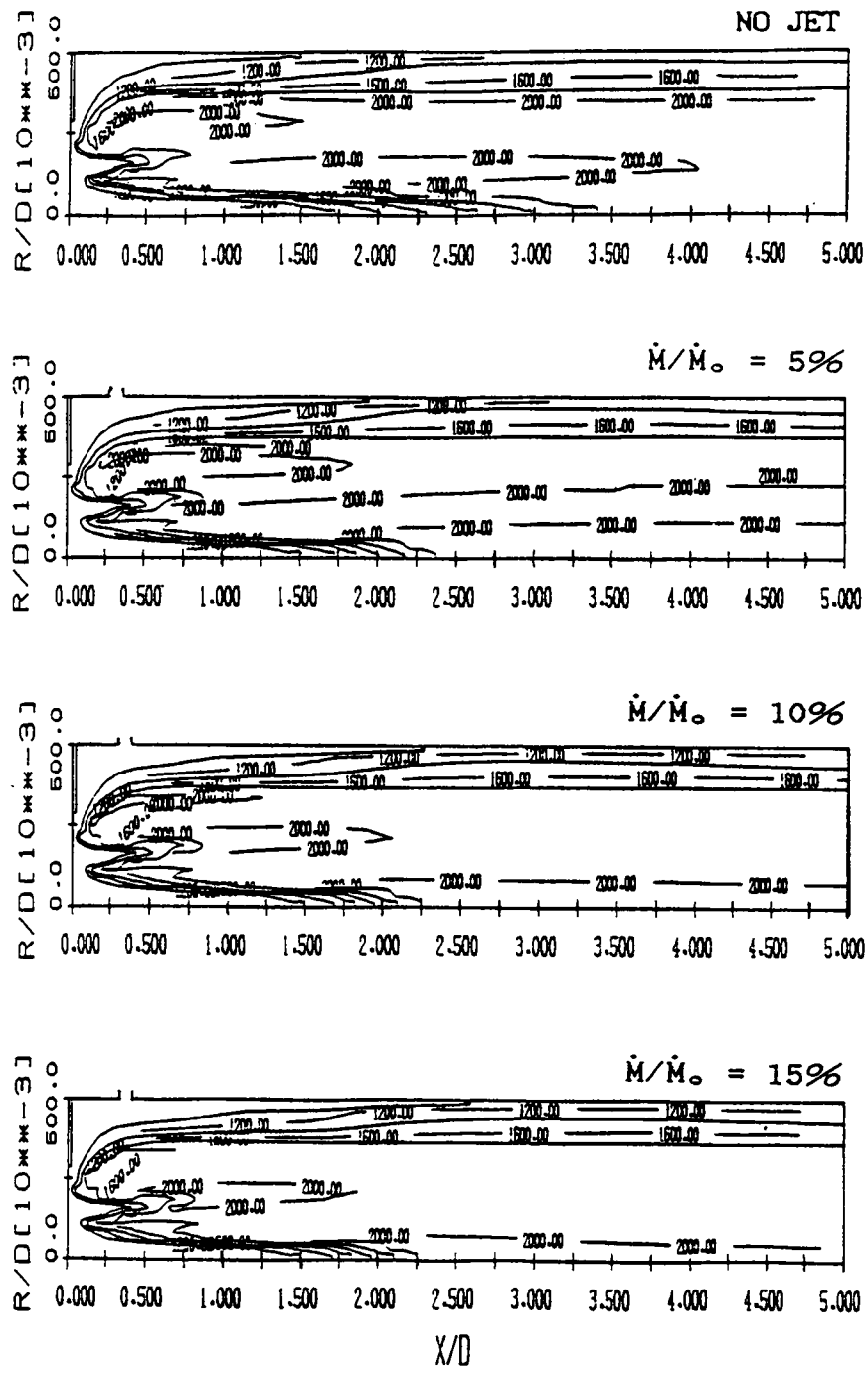

Figure 5. Temperature distributions for different injected mass fractions

temperature is around 2000 K in the intermixing region of air stream and fuel stream. The high-temperature zone around the centreline (i.e. 2000 K) expands towards the centreline when $\dot{M}/\dot{M}_0$ is increased. This is also due to the fact that the greater side-inlet velocity causes better turbulent mixing when $\dot{M}/M_0$ is increased.

Effect of $\dot{M}/\dot{M}_0$ on wall temperature and combustion efficiency

The temperature along the surface of the upper wall for different injected mass fractions when $A/F = 17{\cdot}24$ is shown in Figure 6. With increasing $\dot{M}/\dot{M}_0$ the cooling fluid injected from the side-inlet nozzle will exhaust the heat energy around the wall and the wall temperature will thus decrease. The combustion efficiency also decreases with increasing injected mass fraction, as shown in Figure 7, since the cooling fluid injected will lower the average temperature of the flow field, leading to a decrease in the combustion efficiency of the flow field.

Effects of number of side-inlet nozzles on temperature and turbulence kinectic energy distributions

The temperature distributions with one and four side-inlet nozzles when $\dot{M}/\dot{M}_0 = 5\%$ and $A/F = 17{\cdot}24$ are shown in Figurer 8. Generally speaking, the patterns of temperature and fuel mass fraction distribution are similar; this is due to the fact that the fuel mass fraction contour is the fuel-exhausted position where the fuel is almost fully combusted and reaches the highest temperature. When the number of side-inlet nozzles is four, the turbulence kinetic energy is higher than when the number of side-inlet nozzles is one, as shown in Figure 9. This result is due to the fact that the turbulent mixing is better when the number of side-inlet nozzles is increased.

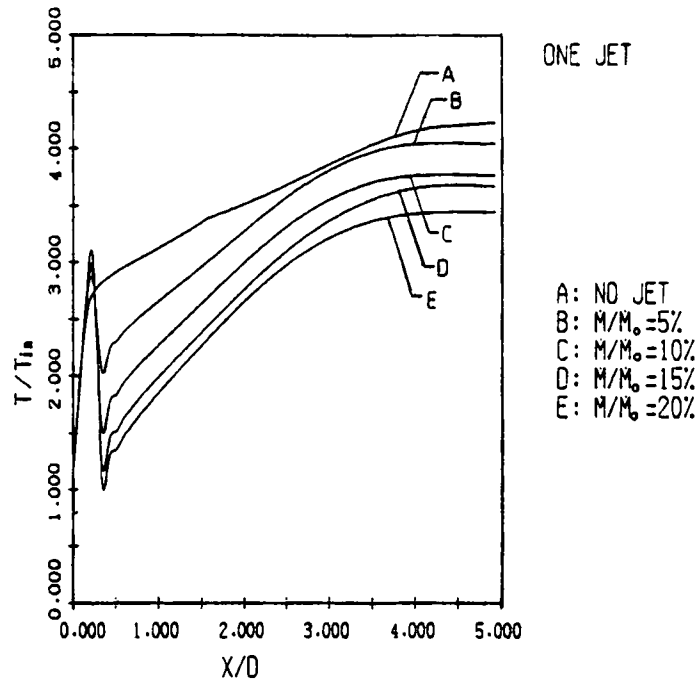

Figure 6. Variation in normalized temperature along the combustor wall; one jet, $A/F = 17{\cdot}24$

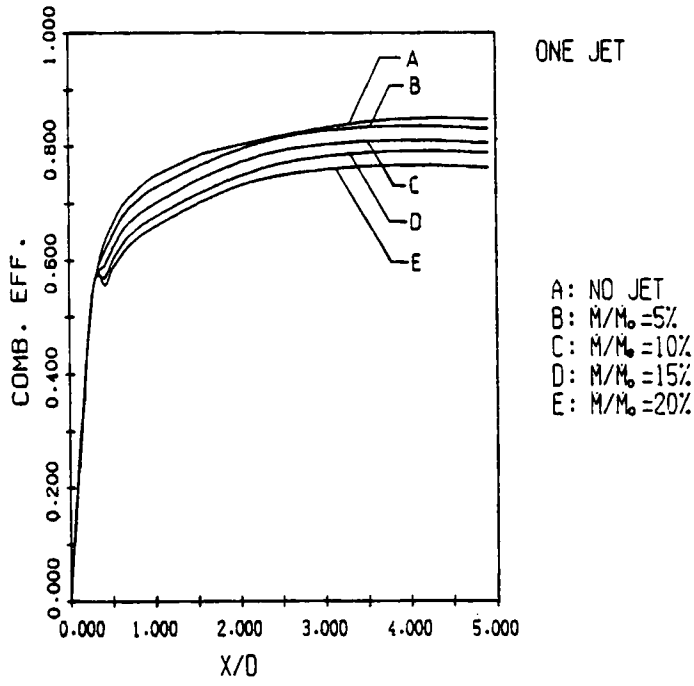

Figure 7. Variation in combustion efficiency along the axial direction; one jet, $A/F = 17{\cdot}24$

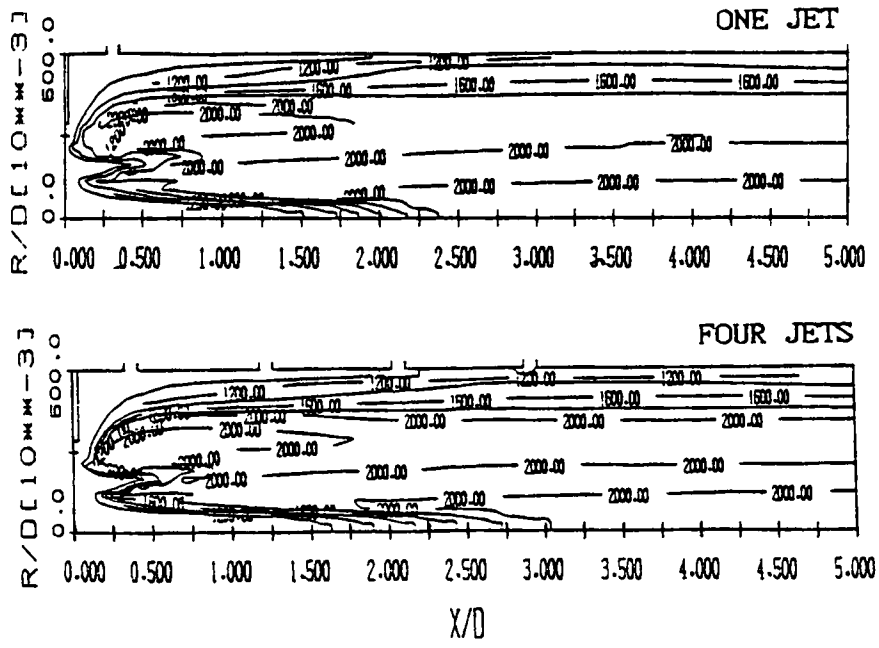

Figure 8. Temperature distributions with different numbers of side-inlet jets

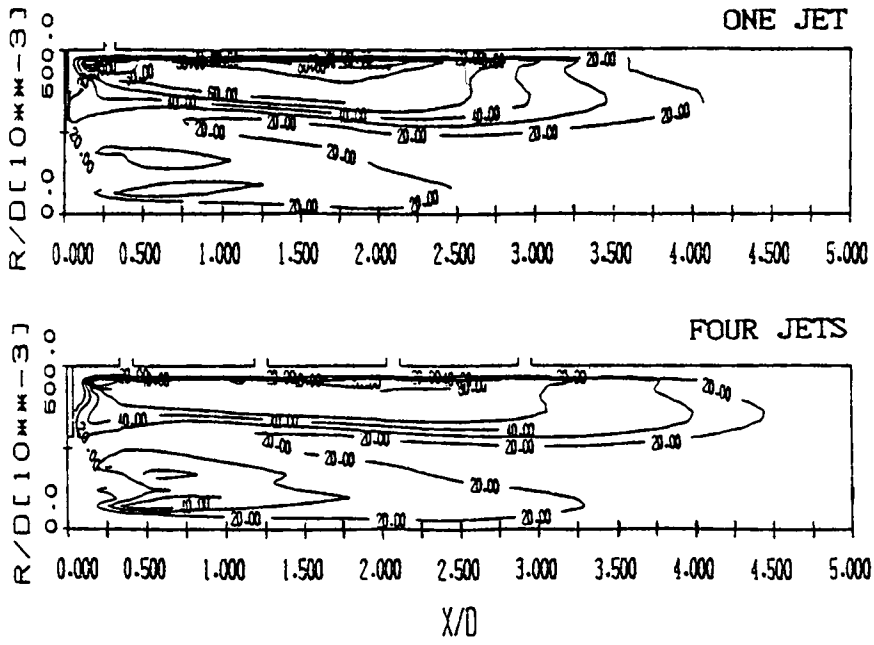

Figure 9. Turbulence kinetic energy distributions with different numbers of side-inlet jets

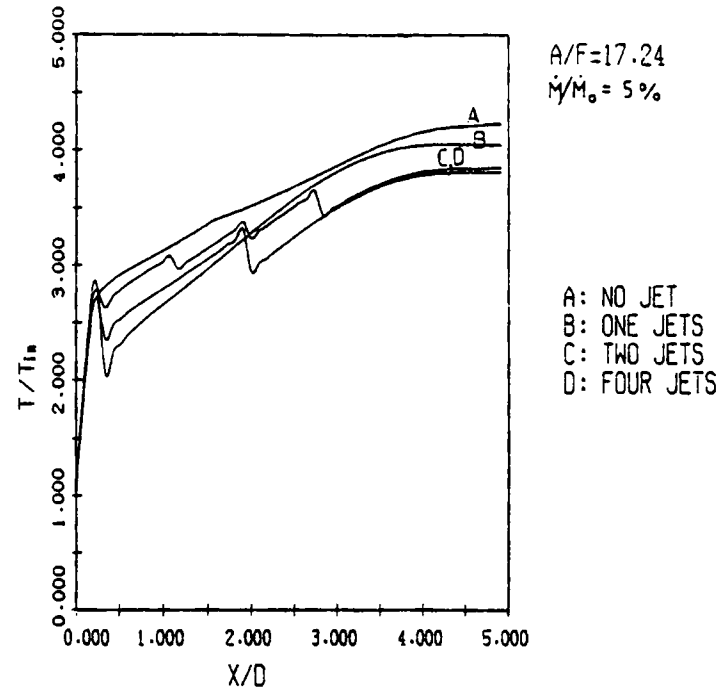

Figure 10. Variation in normalized temperature along the combustor wall; $\dot{M}/\dot{M}_0 = 5\%$, $A/F = 17{\cdot}24$

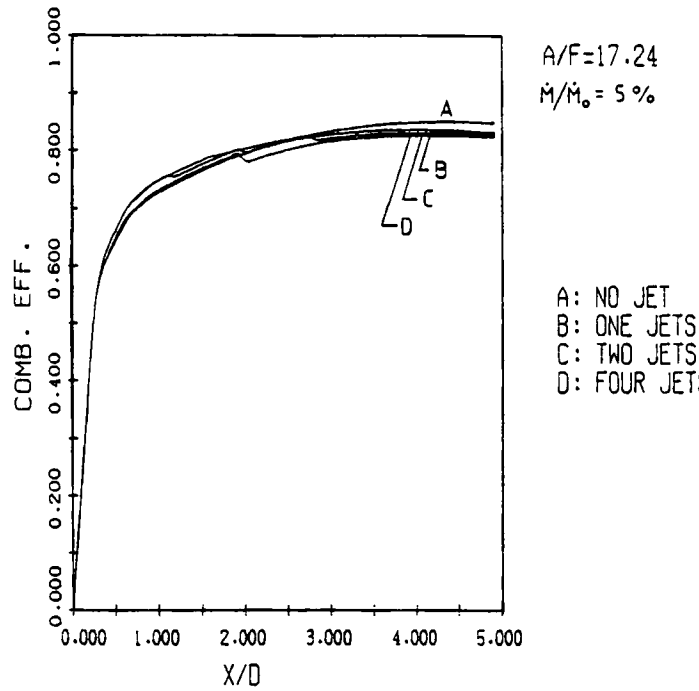

Figure 11. Variation in combustion efficiency along the axial direction, $\dot{M}/\dot{M}_o = 5\%$, $A/F = 17{\cdot}24$

Effects of number of side-inlet nozzles on wall temperature and combustion efficiency

The wall temperature and combustion efficiency as a function of the side-inlet number when $A/F = 17{\cdot}24$ and $\dot{M}/\dot{M}_o = 5\%$ are shown in Figures 10 and 11 respectively. The wall temperature drops most before x/D reaches 2 when the side-inlet number is one, as shown in Figure 10. For $x/D > 2$ the degree of fall in wall temperature is quite close for both two jets and four jets. Figure 11 shows that the combustion efficiency is reduced when cooling fluid is injected from the side-inlet nozzle. However, the number of side-inlet nozzles has only a slight influence on the combustion efficiency.

CONCLUDING REMARKS

From the above discussion and analysis we can conclude as follows ($\dot{M}/\dot{M}_o \leqslant 20\%$)

1. In cold flow the structure of the corner recirculation zone is affected by side-inlet fluid, which changes the location of the reattachment point.
2. Both the turbulence kinetic energy and the turbulent mixing effect are promoted when the injected mass fraction is increased.
3. The high-temperature zone expands towards the centreline when the injected mass fraction is increased.
4. The wall temperature along the combustor decreases when the injected mass fraction is increased.

5. The combustion efficiency decreases when the injected mass fraction is increased.
6. The wall temperature along the combustor decreases when the side-inlet number is increased.
7. The effects of the side-inlet number on the combustion efficiency are slight.

APPENDIX: NOMENCLATURE

A_i	surface area of cell
A/F	air–fuel ratio
a_i	coefficient
C_p	specific heat at constant pressure
D	diameter of combustor
D_i	diameter of combustor inlet
f	underrelaxation factor
H	total enthalpy
k	turbulence kinetic energy
$\dot{M}$	mass flow rate of side-inlet jets
$\dot{M}_o$	mass flow rate of combustor inlet
m_{fo}	modified mass fraction ($=m_{ox}-sm_{fu}$)
m_{fu}, m'_{fu}	mass fraction and reaction rate of fuel
m_{ox}	mass fraction of oxidant
m_{pr}	mass fraction of product
P	static pressure
P'	correction pressure
S^ϕ	source term of ϕ-equation
S_p, S_c	coefficients of linearized source term
s	stoichiometric ratio
T	temperature
u, v	velocities in axial and radial directions
V	volume
x, r	co-ordinates in axial and radial directions
Γ_ϕ	transport coefficient of ϕ-equation
ΔH_{fu}	heat of reaction per unit mass of fuel
ε	dissipation rate of turbulence kinetic energy
μ_e	effective viscosity
μ_l	molecular viscosity
μ_t	eddy viscosity
ρ	fluid density
ϕ	transport variable

Subscripts

E, N, S, W	neighbouring grid points of grid point P
e, n, s, w	control volume face of grid point P
in	inlet property
nb	general neighbouring grid point
P	central grid point of control volume

REFERENCES

1. A. H. Lefebvre, *Gas Turbine Combustion*, McGraw-Hill, New York, 1980.
2. S. V. Patankar, D. K. Basu and S. A. Alpay, 'Prediction of the three-dimensional velocity field of a defected turbulent jet', *ASME J. Fluids Eng.*, **99**, 758–762 (1977).
3. P. Chassaing, J. George, A. Claria and F. Sananes, 'Physical characteristics of subsonic jets in a cros-stream', *J. Fluid Mech.*, **62**, 41–64 (1974).
4. D. Crabb. D. F. G. and Durao and J. H. Whitelaw, 'A round jet normal to a crossflow', *ASME J. Fluids Eng.*, **103**, 142–152 (1981).
5. K. N. Atkinson, E. A. Khan and J. H. Whitelaw, 'Experimental investigation of opposed jets discharging normally into a cross-stream', *J. Fluid Mech.*, **115**, 493–504 (1982).
6. S. H. Chuang, M. H. Chen, S. W. Lii and F. M. Tai, 'Numerical simulation of a twin-jet impingment on a flat plate coupled with cross flow', *Int. j. numer. methods fluids*, **14**, 459–475 (1992).
7. M. Shahaf, Y. Goldman and J. B. Greenberg, 'An investigation of impinging jets in flow with sudden expansion', *Proc. 22nd Israel Ann. Conf. on Aviation and Astronautics*, Israel Ministry of Transport, 1980, pp. 100–106.
8. P. R. Choudhury, 'Characterization of a side dump gas generator ramjet', *AIAA Paper 82-1258*, 1982.
9. S. P. Vanka, F. D. Stull and R. R. Craig, 'Analytical characterization of flow field in side inlet dump combustor', *AIAA Paper 83-1399*, 1983.
10. S. P. Vanka, R. R. Craig and F. D. Stull, 'Mixing, chemical reaction and flow field development in ducted rockets', *AIAA paper 85-1271*, 1985.
11. M. A. Serag-Eldin and D. B. Spalding, 'Computations of three-dimensional gas turbine combustion chamber flows', *ASME J. Eng. Power*, **101**, 326–336 (1979).
12. W. Shyy, M. E. Braaten and S. M. Correa, 'A numerical study of flow in a combustor with dilution holes', *AIAA Paper 86-0057*, 1986.
13. E. Kilik and P. Schmidt, 'A numerical study of coaxial swirl flow with wall mass injection', *AIAA Paper 86-0369*, 1986.
14. J. D. Holdeman, R. Srinivasan and A. Berenfeld, 'Experiments in dilution jet mixing', *AIAA J.*, **22**, 1436–1443 (1984).
15. F. D. Stull, R. R. Craig, G. D. Wtreby and S. P. Vanka, 'Investigation of dual-inlet side-dump combustor using liquid injection', *J. Propuls. Power*, **1**, 83–86 (1985).
16. G. B. Ferrell, K. Aoki and D. G. Lilley, 'Flow visualization of lateral jet injection into swirling crossflow', *AIAA paper 85-0059*, 1985.
17. R. C. Rudoff and G. S. Samuelsen, 'Detailed measurements of velocity, temperature, and soot in a model gas turbine combustor with wall injection', *AIAA Paper 86-0523*, 1986.
18. L. H. Ong, C. B. McMurry and D. G. Lilley, 'Hot-wire measurements of a single lateral jet injected into swirling crossflow', *AIAA Paper 86-0055*, 1986.
19. T. M. Liou and S. M. Wu, 'Flow field in a dual-inlet side-dump combustor', *J. Propuls. Power*, **4**, 53–60 (1988).
20. D. G. Lilley, 'Flowfield modeling in practical combustor: a review', *J. Energy*, **3**, 193–210 (1979).
21. E. E. Khalil, D. B. Spalding and L. H. Whitelaw, 'The calculation of local flow properties in two dimensional furnaces', *Int. J. Heat Mass Transfer*, **18**, 775–791 (1975).
22. D. G. Lilley, 'Primitive pressure-velocity code for the computation of strongly swirling flow', *AIAA J.*, **14**, 749–756 (1976).
23. R. B. Edelman, P. T. Harsha and S. N. Schmotolocha, 'Modeling technique for the analysis of ramjet combustion processes', *AIAA J.*, **19**, 601–609 (1981).
24. G. H. Vatistas, S. Lin, C. K. Kwok and D. G. Lilley, 'Bluff-body flameholder wakes: a simple numerical solution', *AIAA Paper 82-1177*, 1982.
25. H. M. Jang, 'The flow field analysis of sudden expansion dump combustor of the ramjet engine', *M. S. Thesis*, Department of Mechanical Engineering, National Taiwan University, Taipei, 1982.
26. P. T. Harsha and R. B. Edelman, 'Assessment of modular ramjet combustor model', *J. Spacecraft*, **19**, 430–436 (1982).
27. K. D. Jen and Y. P. Su, 'Sudden expansion dump combustor flowfield simulation and analysis with V-gutter flameholder', *Trans. AASRC*, **18**, 13–24 (1985).
28. S. V. Patankar, *Numerical Heat Transfer and Fluid Flow*, Hemisphere, New York, 1980.
29. J. P. van Doormaal and G. D. Raithby, 'Enhancements of the SIMPLE method for predicting incompressible fluid flows', *Numer. Heat Transfer*, **7**, 147–163 (1984).
30. B. R. Latimer and A. Pollard, 'Comparison of pressure–velocity coupling solution algorithm', *Numer. Heat Transfer*, **8**, 635–652 (1985).
31. Z. C. Hong and T. H. Ko, 'A study on the flow field in a 3D side-inlet dump combustor with different side-inlet angles', *The 11th Natl. Conf. on Theoretical and Applied Mechanics*, STAM Taipei, Taiwan 1987, pp. 211–223.
32. B. E. Launder and D. B. Spalding, *Lectures on Mathematical Model of Turbulence*, Academic, London, 1972.
33. L. F. Moon and G. Rudinger, 'Velocity distribution in an abruptly exanding circular duct', *ASME J. Fluids Eng.*, **99**, 226–230 (1977).